Inorg. Chem. **2005**, *44*, 147–157

Dinuclear Zinc(II) Complexes of Tetraiminodiphenol Macrocycles and Their Interactions with Carboxylate Anions and Amino Acids. Photoluminescence, Equilibria, and Structure

Bula Dutta,[†] Pradip Bag,[†] Ulrich Flörke,[‡] and Kamalaksha Nag*[,†]

Department of Inorganic Chemistry, Indian Association for the Cultivation of Science, Jadavpur, Kolkata 700032, India, and Anorganische und Analytische Chemie, Universität Paderborn, D-33098 Paderborn, Germany

Received July 16, 2004

The reaction equilibria $[H_4L]^{2+} + Zn(OAc)_2 \rightleftharpoons [Zn(H_2L)]^{2+} + 2HOAc$ (K_1) and $[Zn(H_2L)]^{2+} + Zn(OAc)_2 \rightleftharpoons [Zn_2L]^{2+} + 2HOAc$ (K_2), involving zinc acetate and the perchlorate salts of the tetraiminodiphenol macrocycles $[H_4L^{1-3}](ClO_4)_2$, the lateral $(CH_2)_n$ chains of which vary between $n = 2$ and $n = 4$, have been studied by spectrophotometric and spectrofluorimetric titrations in acetonitrile. The photoluminescence behavior of the complexes $[Zn_2L^1](ClO_4)_2$, $[Zn_2L^2(H_2O)_2](ClO_4)_2$, $[Zn_2L^2(\mu\text{-}O_2CR)](ClO_4)$ (R = CH_3, C_6H_5, *p*-$CH_3C_6H_4$, *p*-$OCH_3C_6H_4$, *p*-ClC_6H_4, *p*-$NO_2C_6H_4$), and $[Zn_2L^3(\mu\text{-}OAc)](ClO_4)$ have been investigated. The X-ray crystal structures of the complexes $[Zn_2L^2(H_2O)_2](ClO_4)_2$, $[Zn_2L^3(\mu\text{-}OAc)](ClO_4)$, and $[Zn_2L^2(\mu\text{-}OBz)(OBz)(H_3O)](ClO_4)$ have been determined. The complex $[Zn_2L^2(\mu\text{-}OBz)(OBz)(H_3O)](ClO_4)$ in which the coordinated water molecule is present as the hydronium ion (H_3O^+) on deprotonation gives rise to the neutral dibenzoate-bridged compound $[Zn_2L^2(\mu\text{-}OBz)_2]\cdot H_2O$. The equilibrium constants (K) for the reaction $[Zn_2L^2(H_2O)_2]^{2+} + A^- \rightleftharpoons [Zn_2L^2A]^+ + 2H_2O$ (K), where A^- = acetate, benzoate, or the carboxylate moiety of the amino acids glycine, L-alanine, L-histidine, L-valine, and L-proline, have been determined spectrofluorimetrically in aqueous solution (pH 6–7) at room temperature. The binding constants (K) evaluated for these systems vary in the range $(1–8) \times 10^5$.

Introduction

Zinc(II) plays important roles in several biological processes.[1] Apart from enzymes with one zinc binding site, e.g., carbonic anhydrase and carboxypeptidase A, enzymes containing two or three zinc ions at the active sites are also of particular interest.[2] Dinuclear zinc(II) cores are often seen in biological systems, such as phosphatases[3,4] and aminopeptidases.[5,6] In addition, some synthetic dinuclear zinc(II) complexes are found to have functions in RNA hydrolysis[7] and dephosphorylation.[8] The role of zinc in neurobiology is a topic of substantial current interest.[9−11]

To elucidate the role of Zn(II) in such events, detection methods that exhibit selectivity and sensitivity for Zn(II) and are suitable for use in biological fluids are required. However, due to its $3d^{10}$ electronic configuration, the common analytical techniques such as UV−vis, Mössbauer, NMR, and EPR spectroscopy cannot be applied to detect zinc(II) ions in biological systems. Fortunately, fluorescent imaging has been found to be the most powerful technique for this purpose.[12]

* Author to whom correspondence should be addressed. E-mail: ickn@mahendra.iacs.res.in.
[†] Indian Association for the Cultivation of Science.
[‡] Universität Paderborn.

(1) (a) Fraústo da Silva, J. J.; Williams, R. J. P. *The Biological Chemistry of the Elements*; Clarendon Press: Oxford, 1991; p 302. (b) Berg, J. M.; Shi, Yi. *Science* **1996**, *271*, 1081.
(2) (a) Lipscomb, W. N.; Sträter, N. *Chem. Rev.* **1996**, *96*, 2375. (b) Wilcox, D. E. *Chem. Rev.* **1996**, *96*, 2435. (c) Sträter, N.; Lipscomb, W. N.; Klabunde, T.; Crebs, B. *Angew. Chem., Int. Ed. Engl.* **1996**, *35*, 2024. (d) Steinhagen, H.; Helmchem, G. *Angew. Chem., Int. Ed. Engl.* **1996**, *35*, 2339.
(3) Dealwis, C. G.; Chen, L.; Brennan, C.; Mandecki, W.; AbadZaptero, C. *Protein Eng.* **1995**, *8*, 865.
(4) Zhang, Y.; Liang, J. Y.; Huang, H.; Ke, H.; Lipscomb, W. N. *Biochemistry* **1993**, *32*, 7844.
(5) Burley, S. K.; David, P. R.; Taylor, A.; Lipscomb, W. N. *Proc. Natl. Acad. Sci. U.S.A.* **1990**, *87*, 6878.
(6) Roderick, S.; Mathews, B. W. *Biochemistry* **1993**, *32*, 3907.
(7) Ishikubo, A.; Yashiro, M.; Komiyama, M. *Nucleic Acids. Symp. Ser.* **1995**, *34*, 85.
(8) Bazzicalupi, C.; Bencini, A.; Bianchi, A.; Fusi, V.; Giorgi, C.; Paoletti, P.; Valtancoli, B.; Zanchi, D. *Inorg. Chem.* **1997**, *36*, 2784.
(9) Vallee, B. L.; Falchuk, K. H. *Physiol. Rev.* **1993**, *73*, 79.
(10) Frederickson, C. J.; Moncrieff, D. W. *Biol. Signals* **1994**, *3*, 127.
(11) Takeda, A. *BioMetals* **2001**, *14*, 343.
(12) Jiang, P.; Guo, Z. *Coord. Chem. Rev.* **2004**, *248*, 205 and references therein.

10.1021/ic049056a CCC: $30.25
Published on Web 11/25/2004

Chart 1

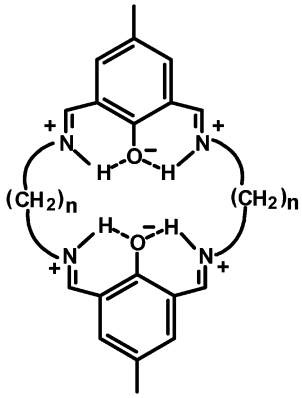

$[H_4L^{1-3}](ClO_4)_2$; n = 2-4

Accordingly, several intensity-based small-molecule fluorescent Zn(II) sensors have been studied that include probes incorporating macrocyclic Zn(II) binding units.[13−16]

In a recent study,[17] we have demonstrated that the perchlorate salts of the tetraiminodiphenol macrocyclic ligands $[H_4L^{1-3}](ClO_4)_2$ (Chart 1) exhibit strong luminescence behavior, albeit there is considerable variation of luminescence intensities along the series. We herein report the luminescence spectroscopic properties of the dinuclear zinc complexes derived from the macrocyclic ligands $[H_4L^{1-3}](ClO_4)_2$. Of particular interest to us has been to examine the fluorophoric behavior of these dizinc complexes toward carboxylate ion binding and to find out whether this approach could be extended to study their interactions with biologically important amino acids. In this context we note that the macrocyclic dinuclear zinc(II) complex $[Zn_2L^2(H_2O)_2](ClO_4)_2$ has been recently used as a precursor to produce interesting structural motifs.[18,19]

Experimental Section

Materials. All chemicals were obtained from commercial sources and used as received. Solvents were purified and dried according to standard methods.[20] The macrocyclic ligands $[H_4L^{1-3}](ClO_4)_2$ were prepared as reported previously.[17]

Caution! *The perchlorate salts reported in this study are potentially explosive and therefore should be handled with care.*[21]

Preparation of the Complexes. $[Zn(H_2L^1)](ClO_4)_2$ (1). To a boiling methanol solution (30 mL) of 4-methyl-2,6-diformylphenol (0.33 g, 2 mmol) were added successively a methanol solution (10 mL) of $Zn(ClO_4)_2\cdot 6H_2O$ (0.36 g, 1 mmol) and a methanol solution (20 mL) of 1,2-diaminoethane (0.12 g, 2 mmol). The resulting bright yellow solution was refluxed for 1 h and then concentrated to a volume of ca. 20 mL. The yellow crystalline compound that was deposited on standing was collected by filtration and washed with methanol and diethyl ether. Yield: 0.54 g (85%). Anal. Calcd for $C_{22}H_{24}N_4O_{10}ZnCl_2$: C, 41.22; H, 3.75; N, 8.74. Found: C, 41.36; H, 3.68; N, 8.57. Selected IR data on KBr (ν/cm^{-1}): 3413br, 2924m, 2856w, 1644s, 1542s, 1492w, 1442m, 1383w, 1335m, 1230m, 1089s, 993m, 876w, 803w, 775w, 687w, 629m, 564w. ^{1}H NMR (300 MHz, CD_3CN): δ 14.62 (s, 2H, N−H···O); 8.61 (d, J = 13.2 Hz, 2H, CH═N); 8.48 (s, 2H, CH═N); 7.62 (s, 2H, Ar); 7.50 (s, 2H, Ar); 4.13 (m, 4H, CH_2); 3.96 (s, 4H, CH_2); 2.14 (s, 6H, CH_3).

$[Zn_2L^1](ClO_4)_2\cdot H_2O$ (2). This compound can be prepared in two ways.

Method I. To a boiling methanol solution (30 mL) of 4-methyl-2,6-diformylphenol (0.33 g, 2 mmol) was added a methanol solution (10 mL) containing $Zn(ClO_4)_2\cdot 6H_2O$ (0.36 g, 1 mmol) and $Zn(OAc)_2\cdot 2H_2O$ (0.22 g, 1 mmol). A methanol solution (20 mL) of 1,2-diaminoethane (0.12 g, 2 mmol) was then added dropwise. The resulting light yellow solution was refluxed for 1 h, after which it was concentrated to ca. 5 mL. The light yellow crystals that were deposited were collected by filtration and washed with methanol and diethyl ether. Yield: 0.57 g (80%).

Method II. To a stirred acetonitrile solution (15 mL) of compound **1** (0.64 g, 1 mmol) was added a second acetonitrile solution (10 mL) of $Zn(OAc)_2\cdot 2H_2O$ (0.22 g, 1 mmol). After 1 h of stirring the solution was concentrated to a small volume, when a light yellow crystalline compound was deposited. The product was filtered and washed with diethyl ether. Yield: 0.59 g (87%). Anal. Calcd for $C_{22}H_{24}N_4O_{11}Zn_2Cl_2$: C, 36.62; H, 3.33; N, 7.77. Found: C, 36.85; H, 3.42; N, 7.72. Selected IR data on KBr (ν/cm^{-1}): 3425br, 3008w, 2926m, 2852w, 1633s, 1547s, 1442m, 1390s, 1327m, 1231m, 1148w, 1089s, 1033m, 992w, 881w, 839m, 773w, 673w, 624m, 573w, 532w. ^{1}H NMR (300 MHz, CD_3CN): δ 8.36 (s, 4H, CH═N); 7.34 (s, 4H, Ar); 4.21 (s, 4H, CH_2); 3.67 (s, 4H, CH_2); 2.24 (s, 6H, CH_3); 2.14 (s, br, H_2O).

$[Zn_2L^2(H_2O)_2](ClO_4)_2$ (3). This compound also can be prepared in two ways.

Method I. To a boiling methanol solution (30 mL) of 4-methyl-2,6-diformylphenol (0.33 g, 2 mmol) and $Zn(ClO_4)_2\cdot 6H_2O$ (0.72 g, 2 mmol) was added a methanol solution (20 mL) of 1,3-diaminopropane (0.15 g, 2 mmol). The resulting deep yellow solution was refluxed for 1 h and then concentrated to a volume of ca. 15 mL. The yellow crystals that were deposited on standing were collected by filtration and washed with methanol and diethyl ether. Yield: 0.62 g (80%).

Method II. To an acetonotrile solution (20 mL) of the macrocycle $[H_4L^2](ClO_4)_2$ (0.60 g, 1 mmol) were added successively acetonitrile solutions (10 mL each) of $Zn(ClO_4)_2\cdot 6H_2O$ (0.72 g, 2 mmol) and Et_3N (0.40 g, 4 mmol). The solution was refluxed for 1 h and concentrated to a volume of ca. 15 mL. The yellow crystalline product that was deposited was filtered off and washed with acetonitrile and diethyl ether. Yield: 0.64 g (83%). Anal. Calcd for $C_{24}H_{30}N_4O_{12}Zn_2Cl_2$: C, 37.51; H, 3.91; N, 7.29. Found: C, 37.38; H, 3.96; N, 7.24. Selected IR data on KBr (ν/ cm^{-1}): 3416br, 2916m, 2859w, 1639s, 1558s, 1439m, 1390m, 1366w, 1330s, 1280m, 1238m, 1118s, 1082s, 982w, 930w, 812m, 629m, 519w. ^{1}H NMR (300 MHz, $(CD_3)_2SO$): δ 8.48 (s, 4H, CH═N); 7.52 (s, 4H, Ar); 3.97 (s, 8H, α-CH_2); 2.27 (s, 6H, CH_3); 2.03 (s, 4H, β-CH_2).

(13) Hirano, T.; Kazuya, K.; Urano, Y.; Higuchi, T.; Nagano, T. *Angew. Chem., Int. Ed.* **2000**, *39*, 1052.
(14) Koike, T.; Watanabe, T.; Aoki, S.; Kimura, E.; Shiro, M. *J. Am. Chem. Soc.* **1996**, *118*, 12696.
(15) Kimura, E.; Koike, T. *Chem. Soc. Rev.* **1998**, *27*, 179 and references therein.
(16) Aoki, S.; Kaido, S.; Fujioka, H.; Kimura, E. *Inorg. Chem.* **2003**, *42*, 1023.
(17) Dutta, B.; Bag, P.; Adhikary, B.; Flörke, U.; Nag, K. *J. Org. Chem.* **2004**, *69*, 5419.
(18) Huang, W.; Gou, S.; Hu, D.; Chantrapromma, S.; Fun, H.-K.; Meng, Q. *Inorg. Chem.* **2001**, *40*, 1712.
(19) Huang, W.; Gou, S.; Hu, D.; Chantrapromma, S.; Fun, H.-K.; Meng, Q. *Inorg. Chem.* **2002**, *41*, 864.
(20) Perrin, D. D.; Armarego, W. L.; Perrin, D. R. *Purification of Laboratory Chemicals*, 2nd ed.; Pergamon: Oxford, 1980.
(21) Wolsey, W. C. *J. Chem. Educ.* **1973**, *50*, A335.

$[Zn_2L^2(\mu\text{-}O_2CR)](ClO_4)\cdot 2H_2O$ (4−9). The following generalized procedure was used to prepare these compounds. To a boiling methanol solution (30 mL) of compound **3** (0.78 g, 1 mmol) was added dropwise a methanol solution (20 mL) of sodium carboxylate salt RCO_2Na (4 mmol). The solution was refluxed for 2 h and then allowed to concentrate slowly on a hot plate. In all of the cases the product was deposited in crystalline form, collected by filtration, and washed with methanol.

Data for $[Zn_2L^2(\mu\text{-}OAc)](ClO_4)\cdot 2H_2O$ (4). Yield: 0.63 g (85%). Anal. Calcd for $C_{26}H_{33}N_4O_{10}Zn_2Cl$: C, 42.95; H, 4.50; N, 7.71. Found: C, 43.01; H, 4.53; N, 7.69. Selected IR data on KBr (ν/cm^{-1}): 3433br, 2918m, 2866w, 1638s, 1580m, 1560s, 1441m, 1411s, 1408m, 1341s, 1280w, 1238m, 1117s, 1085s, 990w, 943w, 813m, 774m, 671w, 629m, 512w. ^{1}H NMR (300 MHz, CD_3CN): δ 8.28 (s, 4H, CH═N); 7.31 (s, 4H, Ar); 4.01 (s, 4H, α-CH_2); 3.82 (s, 4H, α-CH_2); 2.23 (s, 6H, CH_3); 2.15 (s, β-CH_2 + H_2O); 1.80 (s, 3H, OAc).

Data for $[Zn_2L^2(\mu\text{-}OBz)](ClO_4)\cdot 2H_2O$ (5). Yield: 0.62 g (79%). Anal. Calcd for $C_{31}H_{35}N_4O_{10}Zn_2Cl$: C, 47.21; H, 4.44; N, 7.10. Found: C, 47.49; H, 4.60; N, 7.13. Selected IR data on KBr (ν/cm^{-1}): 3433br, 3071w, 2922m, 2859w, 1638s, 1580m, 1560s, 1443m, 1406s, 1331m, 1279w, 1238w, 1116s, 1084s, 990w, 930w, 892w, 813m, 726m, 628m, 512w. ^{1}H NMR (300 MHz, CD_3CN): δ 8.31 (s, 4H, CH═N); 7.96 (d, J = 7.2 Hz, 2H, *o*-C_6H_5); 7.46 (m, 1H, *p*-C_6H_5); 7.37 (m, 2H, *m*-C_6H_5); 7.31 (s, 4H, Ar); 3.99 (s, 8H, α-CH_2); 2.22 (s, 6H, CH_3); 2.14 (s, β-CH_2 + H_2O).

Data for $[Zn_2L^2(\mu\text{-}O_2C\text{-}p\text{-}CH_3C_6H_4)](ClO_4)\cdot 2H_2O$ (6). Yield: 0.64 g (80%). Anal. Calcd for $C_{32}H_{37}N_4O_{10}Zn_2Cl$: C, 47.88; H, 4.61; N, 6.98. Found: C, 48.01; H, 4.54; N, 7.12. Selected IR data on KBr (ν/cm^{-1}): 3424br, 2922m, 2866w, 1637s, 1587m, 1559s, 1444s, 1405s, 1333s, 1278w, 1239m, 1178s, 1087s, 998w, 937w, 814m, 771m, 625m, 519w. ^{1}H NMR (300 MHz, CD_3CN): δ 8.31 (s, 4H, CH═N); 7.85 (d, J = 8.2 Hz, 2H, *o*-C_6H_4); 7.31 (s, 4H, Ar); 7.15 (d, J = 8.0 Hz, 2H, *m*-C_6H_4); 4.08 (s, 4H, α-CH_2); 3.89 (s, 4H, α-CH_2); 2.29 (s, 3H, *p*-CH_3); 2.22 (s, 6H, CH_3); 2.12 (s, β-CH_2 + H_2O).

Data for $[Zn_2L^2(\mu\text{-}O_2C\text{-}p\text{-}OCH_3C_6H_4)](ClO_4)\cdot 2H_2O$ (7). Yield: 0.62 g (76%). Anal. Calcd for $C_{32}H_{37}N_4O_{11}Zn_2Cl$: C, 46.91; H, 4.52; N, 6.84. Found: C, 47.02; H, 4.56; N, 6.87. Selected IR data on KBr (ν/cm^{-1}): 3429br, 3058w, 2928m, 2866w, 1635s, 1604m, 1587m, 1560s, 1450m, 1398s, 1338m, 1248m, 1172m, 1090s, 1030w, 816w, 788m, 711w, 623m, 512w. ^{1}H NMR (300 MHz, CD_3CN): δ 8.31 (s, 4H, CH═N); 7.92 (d, J = 8.7 Hz, 2H, *o*-C_6H_4); 7.32 (s, 4H, Ar); 6.85 (d, J = 8.7 Hz, 2H, *m*-C_6H_4); 4.12 (s, 4H, α-CH_2); 3.87 (s, 4H, α-CH_2); 3.75 (s, 3H, OCH_3); 2.22 (s, 6H, CH_3); 2.12 (s, β-CH_2 + H_2O).

Data for $[Zn_2L^2(\mu\text{-}O_2C\text{-}p\text{-}ClC_6H_4)](ClO_4)\cdot 2H_2O$ (8). Yield: 0.62 g (75%). Anal. Calcd for $C_{31}H_{34}N_4O_{10}Zn_2Cl_2$: C, 45.23; H, 4.13; N, 6.80. Found: C, 45.46; H, 4.01; N, 6.87. Selected IR data on KBr (ν/cm^{-1}): 3433br, 2924m, 2858w, 1637s, 1580m, 1560s, 1445m, 1407s, 1334m, 1278w, 1239w, 1194w, 1086s, 937w, 877w, 816m, 774m, 624m, 559w. ^{1}H NMR (300 MHz, CD_3CN): δ 8.31 (s, 4H, CH═N); 7.94 (d, J = 8.1 Hz, 2H, *o*-C_6H_4); 7.36 (s, 2H, *m*-C_6H_4); 7.32 (s, 4H, Ar); 4.12 (s, 4H, α-CH_2); 3.88 (s, 4H, α-CH_2); 2.22 (s, 6H, CH_3); 2.10 (s, β-CH_2 + H_2O).

Data for $[Zn_2L^2(\mu\text{-}O_2C\text{-}p\text{-}NO_2C_6H_4)](ClO_4)\cdot 2H_2O$ (9). Yield: 0.60 g (72%). Anal. Calcd for $C_{31}H_{34}N_5O_{12}Zn_2Cl$: C, 44.63; H, 4.07; N, 8.39. Found: C, 44.71; H, 4.02; N, 8.56. Selected IR data on KBr (ν/cm^{-1}): 3417br, 2932m, 2872w, 1635s, 1605m, 1573s, 1556s, 1524m, 1450s, 1409s, 1342s, 1275w, 1248m, 1089s, 1009w, 976w, 890w, 822m, 775m, 726m, 623m, 539w, 506w. ^{1}H NMR (300 MHz, CD_3CN): δ 8.31 (s, 4H, CH═N); 8.11 (s, 4H, *o*,*m*-C_6H_4); 7.32 (s, 4H, Ar); 3.99 (s, 8H, α-CH_2); 2.22 (s, 6H, CH_3); 2.12 (s, β-CH_2 + H_2O).

$[Zn_2L^2(\mu\text{-}OBz)(OBz)(H_3O)](ClO_4)$ (10). An acetonitrile solution (40 mL) of **5** (0.20 g, 0.25 mmol) and benzoic acid (0.12 g, 1 mmol) was heated under reflux for 4 h. The color of the solution faded from bright yellow to pale yellow during this period. After the volume of the solution was reduced to ca. 20 mL, it was kept at room temperature in a stoppered flask. The pale yellow crystals that were deposited over a period of 2 days were collected by filtration and washed with methanol and diethyl ether. Yield: 80 mg (35%). Anal. Calcd for $C_{38}H_{39}N_4O_{11}Zn_2Cl$: C, 51.05; H, 4.37; N, 6.27. Found: C, 51.19; H, 4.41; N, 6.18. Selected IR data on KBr (ν/cm^{-1}): 3496br, 3420br, 3071w, 2928m, 2866w, 1653s, 1605m, 1568s, 1443m, 1421m, 1372s, 1327m, 1274w, 1198w, 1086s, 979w, 945w, 810m, 767m, 726m, 677m, 626m, 526w, 460w. ^{1}H NMR (300 MHz, CD_3CN): δ 8.35 (s, 2H, CH═N); 8.30 (s, 2H, CH═N); 7.75 (d, J = 7.4 Hz, 4H, *o*-C_6H_5); 7.38 (s, 4H, Ar); 7.31 (m, 2H, *p*-C_6H_5); 7.25 (m, 4H, *m*-C_6H_5); 4.20 (m, 4H, α-CH_2); 4.07 (m, 4H, α-CH_2); 2.35 (m, 2H, β-CH_2); 2.20 (m, 2H, β-CH_2); 2.17 (s, 6H, CH_3).

$[Zn_2L^2(\mu\text{-}OBz)_2]\cdot H_2O$ (11). Complex **10** (63 mg, 0.07 mmol) was dissolved in 10 mL of warm acetonitrile and treated with 0.8 mL of 0.1 mM NaOH solution. After a few minutes of stirring, the yellow microcrystalline product that was deposited was collected by centrifugation and washed with methanol and diethyl ether. Yield: 50 mg (90%). Anal. Calcd for $C_{38}H_{38}N_4O_7Zn_2$: C, 57.50; H, 4.79; N, 7.06. Found: C, 57.32; H, 4.86; N, 7.11. Selected IR data on KBr (ν/cm^{-1}): 3430br, 3071w, 2916m, 2859w, 1638s, 1559s, 1437m, 1411s, 1348s, 1279m, 1237m, 1202w, 1129w, 1089w, 937w, 811m, 776m, 721m, 677w, 539w. ^{1}H NMR (300 MHz, $(CD_3)_2SO$): δ 8.44 (s, 4H, CH═N); 7.69 (d, J = 7.6 Hz, 4H, *o*-C_6H_5); 7.41 (s, 4H, Ar); 7.33 (m, 2H, *p*-C_6H_5); 7.22 (m, 4H, *m*-C_6H_5); 4.03 (m, 8H, α-CH_2); 3.34 (s, br, H_2O); 2.23 (s, 6H, CH_3); 2.09 (s, 4H, β-CH_2).

$[Zn_2L^3(\mu\text{-}OAc)](ClO_4)$ (12). To an acetonitrile solution (20 mL) of the macrocycle $[H_4L^3](ClO_4)_2$ (0.31 g, 0.5 mmol) was added dropwise with stirring an acetonitrile solution (10 mL) of $Zn(OAc)_2\cdot 2H_2O$ (0.22 g, 1 mmol). After 2 h, the solution was concentrated in a water bath to a small volume, when a yellow crystalline compound separated out. It was collected by filtration and washed with a little methanol and diethyl ether. Yield: 0.40 g (68%). Anal. Calcd for $C_{28}H_{33}N_4O_8Zn_2Cl$: C, 46.76; H, 4.59; N, 7.79. Found: C, 46.40; H, 4.42; N, 7.74. Selected IR data on KBr (ν/cm^{-1}): 3453br, 2937m, 2877w, 1635s, 1604m, 1566s, 1413m, 1408m, 1343m, 1282w, 1223w, 1189w, 1091s, 1017w, 818m, 774w, 623m, 488w. ^{1}H NMR (300 MHz, CD_3CN): δ 8.38 (s, 4H, CH═N); 7.33 (s, 4H, Ar); 3.82−3.64 (m, 8H, α-CH_2); 2.25 (s, 6H, CH_3); 2.03 (m, 8H, β-CH_2); 1.78 (s, 3H, OAc).

Physical Measurements. Elemental (C, H, and N) analyses were performed in-house on a Perkin-Elmer 2400II elemental analyzer. Infrared spectra were recorded on an FT-IR Nexus Nicolet spectrometer using KBr disks. The ^{1}H NMR spectroscopic measurements were performed on a Bruker Avance DPX-300 spectrometer in CD_3CN or $(CD_3)_2SO$ solutions. Electronic absorption spectra were obtained with a Shimadzu UV 2100 spectrophotometer. The spectrophotometric titrations were carried out by recording a series of spectra of acetonitrile solutions of the macrocycles $[H_4L^{1-3}](ClO_4)_2$ mixed with varying quantities of $Zn(OAc)_2\cdot 2H_2O$. The concentration of the ligand was fixed to 10^{-5} M, while that of $Zn(OAc)_2\cdot 2H_2O$ was varied over a wide range till no further change in absorbance was noted.

Emission spectra were recorded on a Perkin-Elmer LS55 luminescence spectrometer using methanol and acetonitrile solutions

Table 1. Crystallographic Data for **3**, **10**, and **12**

	3	**10**	**12**
empirical formula	$C_{24}H_{30}Cl_2N_4O_{12}ZN_2$	$C_{38}H_{38}ClN_4O_{11}Zn_2$	$C_{28}H_{33}ClN_4O_8Zn_2$
fw	768.16	892.91	719.77
T, K	120(2)	203(2)	120(2)
cryst syst, space group	monoclinic, $P2_1/c$	orthorhombic, $Pbca$	monoclinic, $P2_1/n$
a, Å	16.7023(5)	14.970(1)	10.3474(5)
b, Å	12.3131(4)	21.633(3)	19.7720(9)
c, Å	14.4857(5)	23.159(3)	14.7902(7)
α, deg	90	90	90
β, deg	106.121(1)	90	104.991(1)
γ, deg	90	90	90
V, Å^3	2861.94(16)	7500.0(15)	2922.9(2)
Z, ρ_{calcd}, Mg/m^3	4, 1.783	8, 1.582	4, 1.636
μ, mm^{-1}	1.934	1.418	1.790
F(000)	1568	3672	1480
cryst size, mm^3	0.36 × 0.12 × 0.10	0.38 × 0.12 × 0.06	0.35 × 0.30 × 0.20
refinement method	*a*	*a*	*a*
no. of data/restraints/params	7071/4/412	8610/51/504	7203/0/391
no. of reflns [$I > 2\sigma(I)$]	35862	10193	36599
GOF on F^2	0.990	0.872	1.043
final R indices [$I > 2\sigma(I)$]	R1[b] = 0.0334, wR2[c] = 0.0797	R1[b] = 0.0758, wR2[c] = 0.1555	R1[b] = 0.0282, wR2[c] = 0.0728
R indices (all data)	R1 = 0.0425, wR2 = 0.0822	R1 = 0.2588, wR2 = 0.2524	R1 = 0.0326, wR2 = 0.0751

[a] Full-matrix least-squares on F^2. [b] $R1(F) = \sum||F_o| - |F_c||/\sum|F_o|$. [c] $wR2(F^2) = [\sum w(F_o^2 - F_c^2)^2/\sum w(F_o^2)^2]^{1/2}$.

of the complexes. Quantum yields of complexes **3**−**9** at room temperature were determined by a relative method using anthracene as the standard.[22] The quantum yields were calculated using the relation[23]

$$\varphi = \varphi_{std}(A_{std}/A)(I/I_{std})(\eta^2/\eta_{std}^2)$$

where φ and φ_{std} are the quantum yields of unknown and standard samples, A and A_{std} are the solution absorbances at the excitation wavelength (λ_{ex}), I and I_{std} are the integrated emission intensities, and η and η_{std} are the refractive indices of the solvent.

The equlibrium constants involving the binding of acetate or benzoate anions and the carboxylate moieties of amino acids such as glycine, L-alanine, L-histidine, L-valine, and L-proline to $[Zn_2L^2(H_2O)_2]^{2+}$ were determined in aqueous solution at room temperature by spectrofluorimetric titrations. A series of aqueous solutions containing the same amount (1×10^{-5} M) of $[Zn_2L^2(H_2O)_2]^{2+}$ and varying quantities of sodium acetate, sodium benzoate, and the amino acids were added till no further change in luminescence intensity was noted.

Crystal Structure Determination of 3, 10, and 12. Diffraction data were collected on a Siemens R3m/V diffractometer at 120 K (for 3 and 12) and at 203 K (for 10) in the $\omega-2\theta$ scan mode using graphite-monochromated Mo Kα radiation (λ = 0.71073 Å). Pertinent crystallographic data are summarized in Table 1. Three standard reflections were periodically monitored, and no crystal decay was observed. The intensity data were corrected for Lorentz-polarization effects, and semiempirical absorption corrections were made from ψ scans. The structures were solved by direct and Fourier methods and refined by full-matrix least-squares methods based on F^2 using the SHELXTL software package.[24] The non-hydrogen atoms were refined anisotropically, while the hydrogen atoms were placed at the geometrically calculated positions with fixed isotropic thermal parameters.

Results and Discussion

Syntheses. As outlined in Scheme 1, the macrocyclic zinc(II) complexes **1**−**12** have been synthesized either by metal template condensation reaction or using the preformed macrocyclic ligands $[H_4L^{1-3}](ClO_4)_2$.

The cavity sizes of the macrocyclic ligands markedly influence the composition of the zinc(II) complexes formed. Thus, when 2 equiv each of 4-methyl-2,6-diformylphenol and 1,2-diaminoethane are reacted in the presence of 1 equiv of $Zn(ClO_4)_2\cdot 6H_2O$ in methanol, the mononuclear complex $[Zn(H_2L^1)](ClO_4)_2$ (**1**) is obtained. A similar mononuclear complex, however, is not obtained when 1,3-diaminopropane or 1,4-diaminobutane is used as the reactant. On the other hand, the reaction involving equimolar amounts of 4-methyl-2,6-diformylphenol, $Zn(ClO_4)_2\cdot 2H_2O$, and 1,2-diaminoethane or 1,3-diaminopropane produces the dizinc(II) complex $[Zn_2L^1](ClO_4)_2$ (**2**) or $[Zn_2L^2(H_2O)_2](ClO_4)_2$ (**3**), while the same reaction carried out with 1,4-diaminobutane affords the metal-free macrocycle $[H_4L^3](ClO_4)_2$. Again, complex **3** is readily obtained by treating $[H_4L^2](ClO_4)_2$ in acetonitrile with $Zn(ClO_4)_2\cdot 2H_2O$ and triethylamine in a 1:2:4 ratio, albeit similar reactions with $[H_4L^1](ClO_4)_2$ and $[H_4L^3](ClO_4)_2$ fail to produce corresponding dizinc(II) complexes. The dinuclear complex $[Zn_2L^3(\mu\text{-OAc})](ClO_4)$ (**12**) is obtained by reacting $[H_4L^3](ClO_4)_2$ with $Zn(OAc)_2\cdot 2H_2O$ in acetonitrile, even as the same reaction with $[H_4L^2](ClO_4)_2$ produces the acetate-free diaqua complex **3**. A series of carboxylate-bridged compounds $[Zn_2L^2(\mu\text{-}O_2CR)](ClO_4)\cdot 2H_2O$ (**4**−**9**) have been prepared by reacting complex **3** with an excess of NaO_2CR [R = CH_3 (**4**), C_6H_5 (**5**), *p*-$CH_3C_6H_4$ (**6**), *p*-$OCH_3C_6H_4$ (**7**), *p*-ClC_6H_4 (**8**), *p*-$NO_2C_6H_4$ (**9**)] in methanol. Interestingly, the reaction between **5** and benzoic acid in acetonitrile has led to the isolation of an unusual compound of composition $[Zn_2L^2(\mu\text{-OBz})(OBz)(H_3O)](ClO_4)$ (**10**). This compound can be deprotonated to produce the dibenzoate-bridged complex $[Zn_2L^2(\mu\text{-OBz})_2]\cdot H_2O$ (**11**) by treating an acetonitrile solution of **10** with 1 equiv of aqueous sodium hydroxide.

(22) (a) Dawson, W. R.; Windsor, M. W. *J. Phys. Chem.* **1968**, *72*, 3251. (b) Melhuish, W. H. *J. Phys. Chem.* **1961**, *65*, 229. (c) Parker, C. A.; Rees, W. T. *Analyst* **1960**, *85*, 587.
(23) van Houten, J.; Watts, R. J. *J. Am. Chem. Soc.* **1976**, *98*, 4853.
(24) Sheldrick, G. M. *SHELXTL97-2: Program for the Refinement of Crystal Structures*; University of Göttingen: Göttingen, Germany, 1997.

Scheme 1[a]

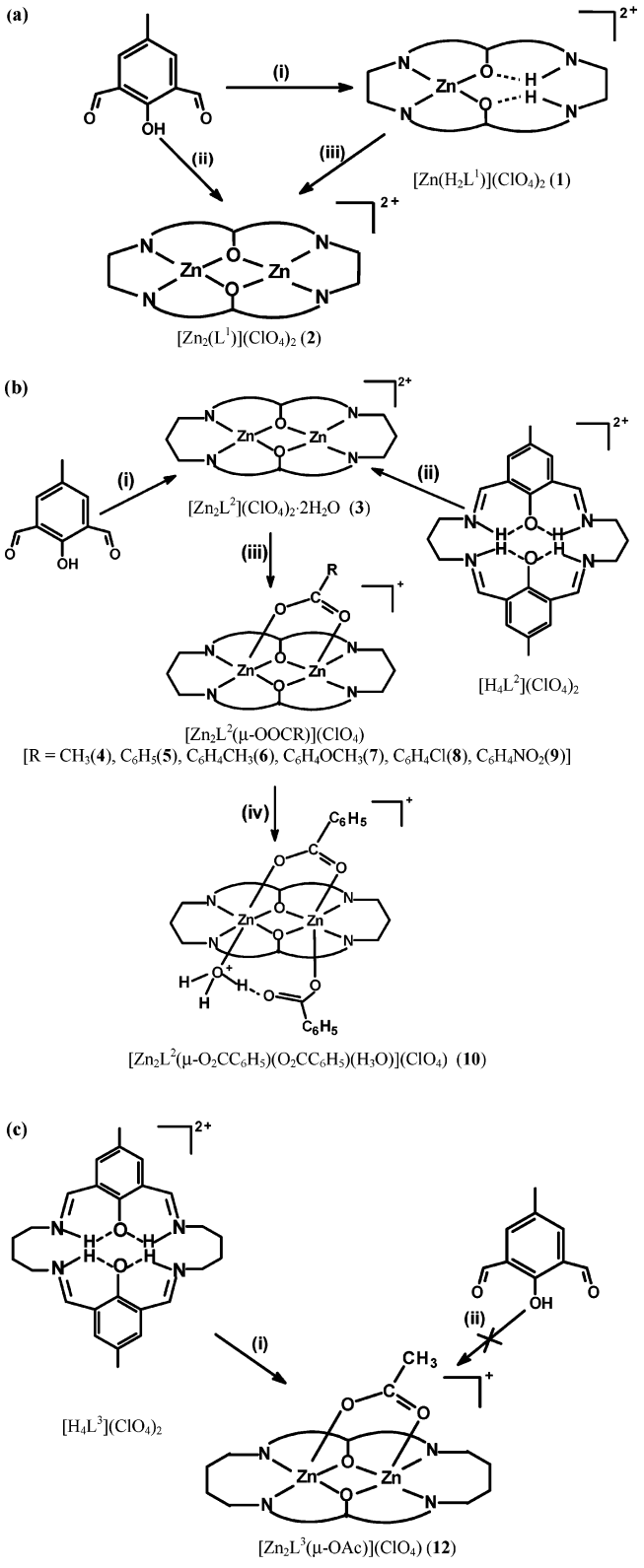

[a] Reagents and conditions: (a) (i) $Zn(ClO_4)_2 \cdot 6H_2O$ (0.5 equiv) + $NH_2(CH_2)_2NH_2$ (1 equiv)/MeOH. (ii) $Zn(ClO_4)_2 \cdot 6H_2O$ (0.5 equiv) + $Zn(OAc)_2 \cdot 2H_2O$ (0.5 equiv) + $NH_2(CH_2)_2NH_2$ (1 equiv)/MeOH. (iii) $Zn(OAc)_2 \cdot 2H_2O$ (1 equiv)/MeCN. (b) (i) $Zn(ClO_4)_2 \cdot 6H_2O$ (1 equiv) + $NH_2(CH_2)_3NH_2$ (1 equiv)/MeOH. (ii) $Zn(ClO_4)_2 \cdot 6H_2O$ (2 equiv) + Et_3N (4 equiv)/MeCN. (iii) NaOOCR (4 equiv)/MeOH. (iv) C_6H_5COOH (4 equiv)/MeCN. (c) (i) $Zn(OAc)_2 \cdot 2H_2O$ (2 equiv)/MeCN. (ii) $Zn(OAc)_2 \cdot 2H_2O$ (1 equiv) + $NH_2(CH_2)_4NH_2$ (1 equiv)/MeOH.

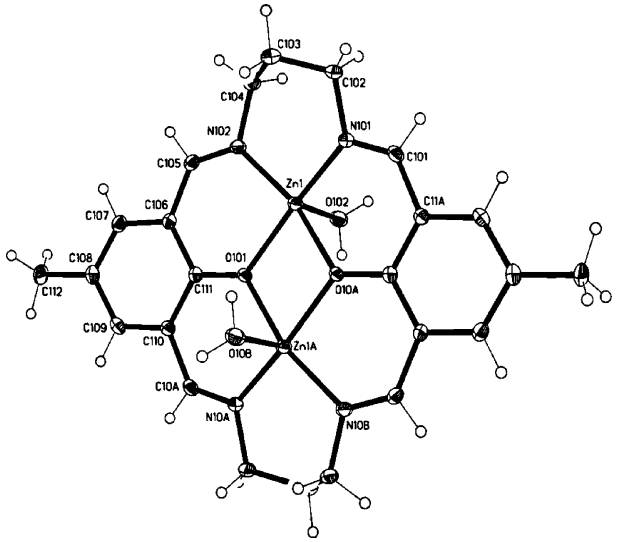

Figure 1. ORTEP representation of the structure of the $[Zn_2L^2(H_2O)_2]^{2+}$ cation in **3**.

Table 2. Selected Bond Lengths (Å) and Angles (deg) for **3**

Zn(1)−N(101)	2.0314(18)	Zn(2)−N(201)	2.0291(19)
Zn(1)−N(102)	2.0236(18)	Zn(2)−N(202)	2.0370(18)
Zn(1)−O(101)	2.0422(15)	Zn(2)−O(201)	2.0589(14)
Zn(1)−O(101)#1	2.0487(15)	Zn(2)−O(201)#2	2.0291(15)
Zn(1)−O(102)	2.0866(17)	Zn(2)−O(202)	2.1123(17)
O(101)−Zn(1)#1	2.0487(15)	O(201)−Zn(2)#2	2.0291(15)
Zn(1)···Zn(1)#1	3.171(1)	Zn(2)···Zn(2)#2	3.175(1)
N(102)−Zn(1)−N(101)	98.51(7)	N(201)−Zn(2)−N(202)	97.76(7)
N(102)−Zn(1)−O(101)	90.52(7)	N(202)−Zn(2)−N(201)	89.65(7)
N(101)−Zn(1)−O(101)	163.44(6)	N(201)−Zn(2)−O(201)	160.73(7)
N(102)−Zn(1)−O(101)#1	164.25(7)	N(202)−Zn(2)−O(201)#2	163.62(6)
N(101)−Zn(1)−O(101)#1	89.83(7)	N(201)−Zn(2)−O(201)#2	90.84(7)
O(101)−Zn(1)−O(101)#1	78.38(6)	O(201)−Zn(2)−O(201)#2	78.07(6)
N(102)−Zn(1)−O(102)	96.63(7)	N(202)−Zn(2)−O(202)	97.90(7)
N(101)−Zn(1)−O(102)	102.22(7)	N(201)−Zn(2)−O(202)	103.63(7)
O(101)−Zn(1)−O(102)	90.40(6)	O(201)−Zn(2)−O(202)	92.86(6)
O(101)#1−Zn(1)−O(102)	90.60(6)	O(201)#2−Zn(2)−O(202)	93.54(6)

Crystal Structures. $[Zn_2L^2(H_2O)_2](ClO_4)_2$ (3). The structure analysis showed that in **3** there are two independent molecules per asymmetric unit. An ORTEP representation for one of the $[Zn_2L^2(H_2O)_2]^{2+}$ cations is shown in Figure 1. Selected bond distances and bond angles are given in Table 2. The cation is centrosymmetric with its center of inversion at the middle of the $Zn_2(\mu$-phenoxide$)_2$ plane. In this compound the flatness of the macrocyclic ligand is evident from the 0° dihedral angle between the two phenyl rings.

For the $[Zn(1)L^2Zn(1A)]^{2+}$ cation, the in-plane donor atoms (N_2O_2) do not deviate from the mean plane by more than 0.004(2) Å, while for the $[Zn(2)L^2Zn(2A)]^{2+}$ cation the deviation is ±0.039(2) Å. The metal centers are displaced from the basal plane in the opposite direction by 0.223(2) Å for Zn(1)/Zn(1A) and 0.260(3) Å for Zn(2)/Zn(2A). The square-pyramidal geometry of the metal center is completed by coordination with a water molecule. The average in-plane Zn−O and Zn−N distances, which lie in the range 2.024−2.049 Å, are normal and the axial Zn−OH_2 distance, 2.089(2) Å, is relatively longer. The separations between the nonbonded metal centers are 3.171 Å for Zn(1)···Zn(1A) and 3.175 Å for Zn(2)···Zn(2A).

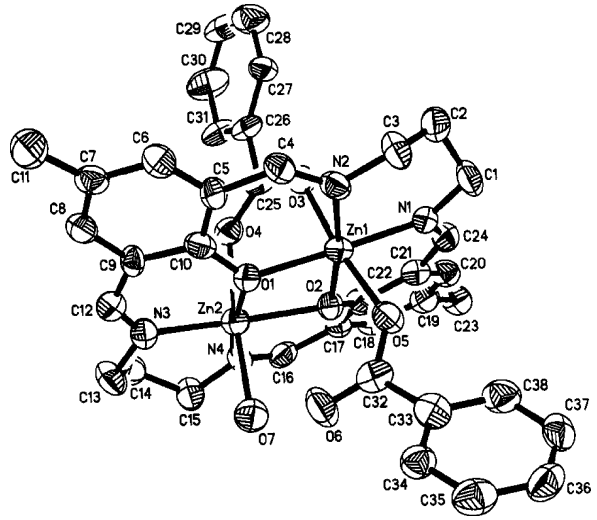

Figure 2. ORTEP representation of the structure of the $[Zn_2L^2(\mu\text{-OBz})(OBz)(H_3O)]^+$ cation in **10**. Hydrogen atoms are not shown for the sake of clarity.

Table 3. Selected Bond Lengths (Å) and Angles (deg) for **10**

Zn(1)−O(1)	2.020(7)	Zn(2)−O(1)	2.076(7)
Zn(1)−O(2)	2.006(7)	Zn(2)−O(2)	2.099(7)
Zn(1)−O(3)	2.035(7)	Zn(2)−O(4)	2.109(7)
Zn(1)−O(5)	1.987(7)	Zn(2)−O(7)	2.153(7)
Zn(1)−N(1)	2.036(8)	Zn(2)−N(3)	2.012(9)
Zn(1)−N(2)	2.049(9)	Zn(2)−N(4)	2.031(9)
Zn(1)···Zn(2)	3.098(1)		
Zn(1)−O(1)−Zn(2)	98.3(3)	Zn(1)−O(2)−Zn(2)	98.0(3)
O(1)−Zn(1)−N(1)	172.0(3)	O(1)−Zn(2)−N(3)	90.8(3)
O(2)−Zn(1)−N(1)	91.5(3)	O(2)−Zn(2)−N(3)	169.6(3)
O(1)−Zn(1)−N(2)	90.5(3)	O(1)−Zn(2)−N(4)	170.3(3)
O(2)−Zn(1)−N(2)	172.8(3)	O(2)−Zn(2)−N(4)	91.1(3)
N(1)−Zn(1)−N(2)	94.9(4)	N(3)−Zn(2)−N(4)	98.9(4)
O(5)−Zn(1)−O(3)	173.0(3)	O(4)−Zn(2)−O(7)	174.3(3)

$[Zn_2L^2(\mu\text{-OBz})(OBz)(H_3O)](ClO_4)$ (10). Complex **10** consists of a protonated cation, $[Zn_2L^2(\mu\text{-OBz})(OBz)(H_2O)]^+$, and a ClO_4 anion in 1:1 stoichiometry. The perchlorate anion is disordered with three of its oxygen atoms distributed over two sites in 2:1 occupancies. The ORTEP diagram of the cation is shown in Figure 2, and the selected bond distances and angles are given in Table 3.

The two metal centers in **10** are triply bridged by the two phenolate oxygens of the macrocyclic ligand and a benzoate group. Both the metal centers are hexacoordinated; the sixth coordination position of Zn(1) is occupied by a monodentate benzoate, while that of Zn(2) is occupied by a water molecule. Unlike **3**, the macrocyclic ligand in **10** adopts a puckered configuration in which the interplanar angle between the planes of the two aromatic rings is 30.1°. The equatorial donor atoms (N_2O_2) do not deviate by more than 0.025 Å from their metal planes. On the other hand, Zn(1) is displaced above the basal plane by 0.078 Å, while Zn(2) lies below the plane by 0.027 Å. The two metal centers are separated from each other by 3.098 Å. Consideration of the metrical parameters for the two metal centers will indicate that, although Zn(1) has a regular octahedral geometry, there is considerable distortion in the geometry of the six-coordinate Zn(2).

The most striking feature of compound **10** is its composition. Although $[Zn_2L^2(\mu\text{-OBz})(OBz)(H_2O)]$ should be a neutral compound, it is, indeed, monocationic, and the charge is neutralized by the associated perchlorate anion. From the structural parameters (Table 3) it is evident that there is no scope for protonation of the macrocyclic ligand donor atoms and also of the carboxylate moieties. We are, therefore, left with two possibilities, namely, either the water molecule is protonated, that is, $[Zn_2L^2(\mu\text{-OBz})(OBz)(H_3O)](ClO_4)$, or the proton is associated with the perchlorate anion, that is, $[Zn_2L^2(\mu\text{-OBz})(OBz)(H_2O)]\cdot HOClO_3$. Interestingly, a macrocyclic zinc(II) complex of composition $[Zn\{[12]aneN_3\}(OH)]_3(ClO_4)_3\cdot HClO_4$ has been structurally characterized.[25] With the crystallographic data set of **10** it has not been possible to determine the hydrogen positions in question. Nevertheless, with HFIX of SHELX we have tried to fix three hydrogen atoms to O(7) or one to O(11) (the only perchlorate oxygen which is not disordered and the only one that due to its orientation could make hydrogen bridge to O(7)). So, if we have $ZnOH_3^+$, there could be an intramolecular bridge, O(7)−H(7B)···O(6), with O(7)−H = 0.83 Å, H···O(6) = 1.77 Å, and O−H···O = 177°, and also an intermolecular bridge, O(7)−H(7C)···O(11), with O(7)−H = 0.83 Å, H···O(11) = 2.25 Å, and O−H···O = 170°. On the other hand, if we have O_3ClOH, there could be intermolecular bridges O(11)−H(11)···O(7) with O−H = 0.83 Å, H···O(7) = 2.53 Å, and O−H···O = 123° and O(11)−H(11)···N(4) with O−H = 0.83 Å, H···N(4) = 2.61 Å, and O−H···N = 118°. In the above-mentioned [12]aneN$_3$ complex,[25] the hydrogen positions were not determined but guessed. The argument for O_3ClOH in that case was a larger Cl−OH bond compared to the other Cl−O bonds. In our case the Cl−O(H) bond in question is just the shortest bond. Thus, the geometric parameters for a Zn−OH_3^+ interaction seems to be the more likely case, as there is no privilege for a ClOH option.

It may be noted that all the Zn(1)−O distances involving the phenolate oxygens [Zn(1)−O(1) = 2.020(7) Å, Zn(1)−O(2) = 2.006(7) Å], the bridged benzoate oxygen [Zn(1)−O(3) = 2.035(7) Å], and the monodentate benzoate oxygen [Zn(1)−O(5) = 1.987(7) Å] are rather short. In contrast, the Zn(2)−O distances involving the phenolate oxygens [Zn(2)−O(1) = 2.076(7) Å, Zn(2)−O(2) = 2.099(7) Å], the bridged benzoate oxygen [Zn(2)−O(4) = 2.109(7) Å], and the water molecule [Zn(2)−O(7) = 2.153(7) Å] are relatively longer. The Zn−N distances for the two metal centers [2.012(9)−2.049(9) Å], however, do not show much difference. If we consider that the coordinated oxygen O(7) is associated with OH_3^+, rather than H_2O, migration of electron density from Zn(1) to Zn(2) through the bridging oxygen atoms should occur. Clearly, this will lead to shortening of the Zn(1)−O distances compared to the Zn(2)−O distances. Further, the carbonyl oxygen O(6) of the monodentate benzoate lies on the same side of the protonated water molecule. The 2.592 Å separation between O(6) and O(7) atoms indicates the presence of a moderate to strong hydrogen-bonding interaction.

(25) Kimura, E.; Shiota, T.; Koike, T.; Shiro, M.; Kodama, M. *J. Am. Chem. Soc.* **1990**, *112*, 5805.

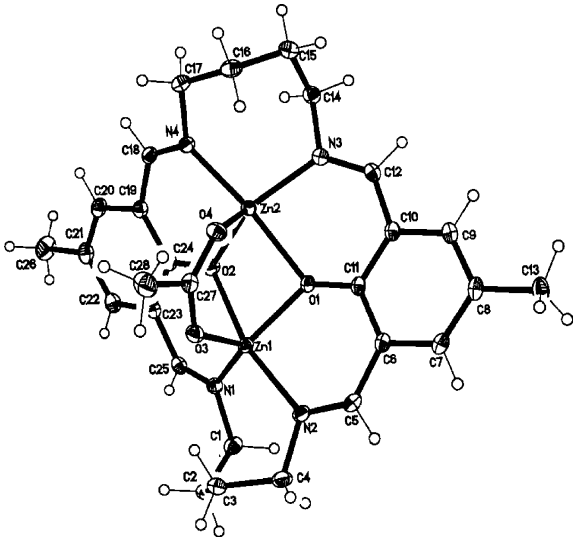

Figure 3. ORTEP representation of the structure of the $[Zn_2L^3(\mu\text{-OAc})]^+$ cation in **12**.

Table 4. Selected Bond Lengths (Å) and Angles (deg) for **12**

Zn(1)−O(1)	1.9875(12)	Zn(2)−O(1)	2.1511(12)
Zn(1)−O(2)	2.1140(12)	Zn(2)−O(2)	1.9772(12)
Zn(1)−O(3)	1.9978(13)	Zn(2)−O(4)	1.9990(13)
Zn(1)−N(1)	2.0376(14)	Zn(2)−N(3)	2.0141(14)
Zn(1)−N(2)	2.0768(14)	Zn(2)−N(4)	2.0620(14)
Zn(1)···Zn(2)	3.039(1)		
Zn(1)−O(1)−Zn(2)	94.41(5)	Zn(1)−O(2)−Zn(2)	95.88(5)
O(1)−Zn(1)−N(1)	132.07(6)	O(1)−Zn(2)−N(3)	85.15(5)
O(2)−Zn(1)−N(1)	84.71(5)	O(2)−Zn(2)−N(3)	135.56(6)
O(1)−Zn(1)−N(2)	90.46(5)	O(1)−Zn(2)−N(4)	163.52(5)
O(2)−Zn(1)−N(2)	165.03(6)	O(2)−Zn(2)−N(4)	90.60(5)
N(1)−Zn(1)−N(2)	100.72(6)	N(3)−Zn(2)−N(4)	99.96(6)
O(1)−Zn(1)−O(3)	103.40(5)	O(1)−Zn(2)−O(4)	91.95(5)
O(2)−Zn(1)−O(3)	91.61(5)	O(2)−Zn(2)−O(4)	101.20(5)

$[Zn_2L^3(\mu\text{-OAc})](ClO_4)$ (12). An ORTEP representation of the cation $[Zn_2L^3(\mu\text{-OAc})]^+$ is shown in Figure 3. Selected bond lengths and angles are listed in Table 4.

The structure consists of two five-coordinated zinc centers, which are bridged by two phenoxide oxygens and the acetate moiety. Due to puckering of the two C_4-linkers, the planes of the two phenyl rings of the macrocycle subtend an angle of 28.6°. The equatorial donor atoms O(1), O(2), N(1), and N(2) for Zn(1) deviate from the mean plane by ±0.282(1) Å, while the atoms O(1), O(2), N(3), and N(4) providing the basal plane for Zn(2) deviate from the least-squares plane by ±0.233(1) Å. The metal centers Zn(1) and Zn(2), in turn, are displaced in the same direction from their mean planes by 0.483(1) and 0.470(1) Å, respectively. The distorted square-pyramidal geometry of the two metal centers is reflected in their relevant bond lengths, which show non-uniformity. The nonbonded Zn(1)···Zn(2) separation is 3.0389(3) Å.

^{1}H NMR Spectra. The proton NMR spectrum of all the complexes, except for **3** and **11**, was obtained in CD_3CN; for **3** and **11** their $(CD_3)_2SO$ solutions were used. The spectrum of the mononuclear complex **1** differs significantly from that of the dinuclear complex **2**. For example, in **1** a low-field resonance is observed at 14.62 ppm due to the hydrogen-bonded N−H···O protons. There are two CH═N resonances at 8.61 and 8.48 ppm for this compound, one of which observed at 8.61 ppm is a doublet (J = 13.2 Hz) due to its *trans* coupling with the hydrogen-bonded proton. Further, the aromatic protons are also nonequivalent and observed at 7.62 and 7.50 ppm. In contrast, the singlets due to the CH═N and aromatic protons of **2** are observed at 8.36 and 7.34 ppm, respectively. The assignment of the 14.62 ppm resonance for **1** has been confirmed by a deuteration experiment. Thus, addition of D_2O to the CD_3CN solution of **1** has led to the disappearance of the 14.62 ppm resonance along with a collapse of the doublet at 8.61 ppm to a broad singlet. The significant deshielding of this resonance is a clear indication of the hydrogen-bonding interaction.

The spectral features of the macrocyclic ligand L^2 in the carboxylate-bridged complexes **4**−**9** remain practically unchanged for all the compounds. For example, the singlets due to the CH═N, OAr, and CH_3 moieties are all observed at 8.31, 7.31, and 2.22 ppm, respectively. Of course, complexes **5**−**9** exhibit additional peaks due to the aromatic carboxylate moieties. Of particular interest to us has been to compare the ^{1}H NMR spectral features of **10** and **11** (shown in Figures S1 and S2 in the Supporting Information). The observation of two singlets of equal intensities at 8.35 and 8.30 ppm due to the imino protons and two multiplets of equal areas at 4.20 and 4.07 ppm due to the α-CH_2 protons in **10** is consistent with its asymmetric structure. The more shielded resonances are for the Zn(2) site. In contrast, complex **11** exhibits a lone singlet at 8.44 ppm for all the CH═N protons and a single resonance at 4.03 ppm for all the α-CH_2 protons, indicating that the two metal centers are in identical environments and both the benzoates are bound in bridged form.

The formation of **11** via deprotonation of **10** has been further verified by comparing their IR spectra (shown in Figures S3 and S4 in the Supporting Information). While the $\nu_{C=N}$ vibration in **10** is split into two components at 1653 and 1605 cm^{-1}, in the case of **11** a single band is observed at 1638 cm^{-1}. Moreover, the asymmetric and symmetric ν_{COO^-} vibrations in **10** are observed at 1568 and 1372 cm^{-1}, as against those observed at 1559 and 1348 cm^{-1} for **11**. More importantly, the ClO_4^- vibrations observed at 1086 and 626 cm^{-1} in **10** are absent in **11**.

Spectrophotometric Titrations of $[H_4L^{1-3}](ClO_4)_2$ with $Zn(OAc)_2\cdot 2H_2O$. The reaction equilibria involving the macrocyclic ligands $[H_4L^{1-3}](ClO_4)_2$ and $Zn(OAc)_2\cdot 2H_2O$ in acetonitrile have been followed spectrophotometrically by observing the spectral changes that occur on the incremental addition of the metal ion to the ligand solution till no further change is noted. As shown in Figure 4, the absorption peak of the ligand $[H_4L^1](ClO_4)_2$ at 450 nm becomes blue-shifted with diminution of intensity on the addition of the metal salt. The successive absorption curves pass through an isosbestic point at 428 nm with the development of a new band at 400 nm, whose intensity becomes maximized when the ligand-to-metal ratio reaches 1:0.6. However, with further addition of the metal salt the intensity of the band at 400 nm becomes depleted at the expense of the growth of another new band at 370 nm, the intensity of which increases until the ligand-to-metal ratio reaches 1:2, beyond which no further change

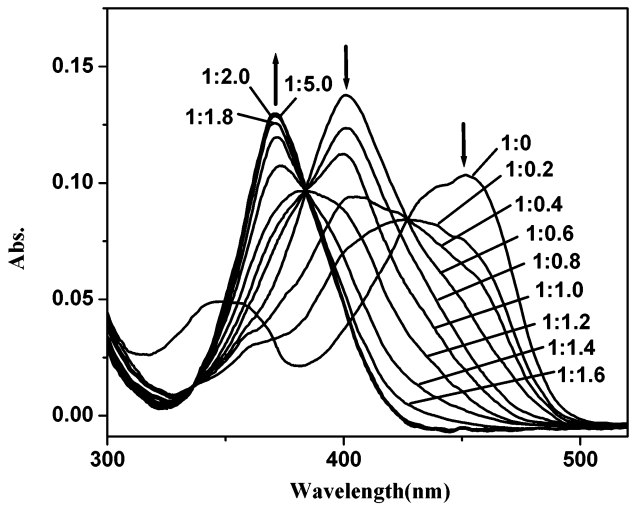

Figure 4. Spectrophotometric titration of the macrocycle $[H_4L^1](ClO_4)_2$ (1×10^{-5} M) with various numbers of equivalents of $Zn(OAc)_2 \cdot 2H_2O$ in acetonitrile.

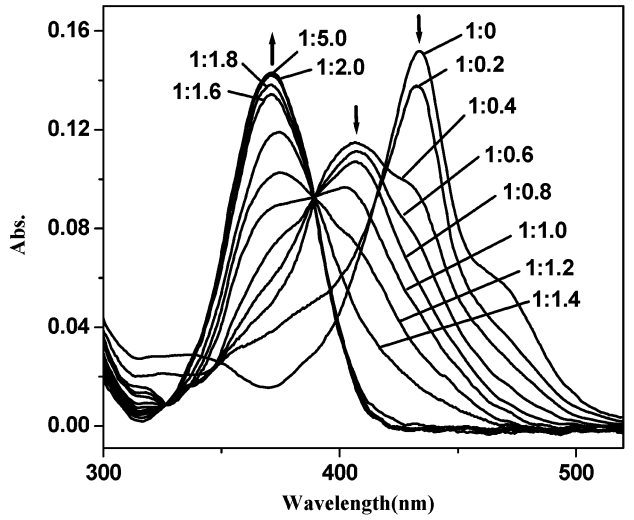

Figure 5. Spectrophotometric titration of the macrocycle $[H_4L^2](ClO_4)_2$ (1×10^{-5} M) with various numbers of equivalents of $Zn(OAc)_2 \cdot 2H_2O$ in acetonitrile.

occurs. During the interval of addition of 0.6−2 equiv of the metal ion, the absorption curves pass through an isosbestic point at 384 nm, while for the entire range of ligand-to-metal ratios all the absorption curves pass through 335 nm. It is important to note that the mononuclear complex **1** in acetonitrile exhibits a band at 400 nm (15600 M^{-1} cm^{-1}), whereas for the dinuclear complex **2** the absorption band is shifted to 370 nm (13900 M^{-1} cm^{-1}). Clearly, the following reaction equilibria are established in solution:

$$[H_4L^1]^{2+} + Zn(OAc)_2 \overset{K_1}{\rightleftharpoons} [Zn(H_2L^1)]^{2+} + 2HOAc \quad (1)$$

$$[Zn(H_2L^1)]^{2+} + Zn(OAc)_2 \overset{K_2}{\rightleftharpoons} [Zn_2L^1]^{2+} + 2HOAc \quad (2)$$

The spectral changes that take place on titrating $[H_4L^2](ClO_4)_2$ with $Zn(OAc)_2 \cdot 2H_2O$ in acetonitrile are shown in Figure 5. Barring the ligand-to-metal ratio of 1:0.2, with increasing amount of metal ion added all the absorption curves pass through two isosbestic points at 390 and 327 nm. During this process the absorption peak at 405 nm continually diminishes in intensity, and at its expense a new band at 370 nm grows. When the metal-to-ligand ratio reaches 1:2, the absorption spectrum resembles that of **3**. Although similar to $[H_4L^1]^{2+}$ here also stepwise reaction equilibrium eqs 3 and 4 are involved, compared to the previous case the two equilibrium constants are more overlapping in the present case. Failure to isolate the mononuclear species $[Zn(H_2L^2)](ClO_4)_2$ is consistent with this observation.

$$[H_4L^2]^{2+} + Zn(OAc)_2 \overset{K_1}{\rightleftharpoons} [Zn(H_2L^2)]^{2+} + 2HOAc \quad (3)$$

$$[Zn(H_2L^2)]^{2+} + Zn(OAc)_2 \overset{K_2}{\rightleftharpoons} [Zn_2L^2]^{2+} + 2HOAc \quad (4)$$

The spectrophotometric titration carried out with $[H_4L^3]^{2+}$ (Figure S5 in the Supporting Information) shows that with increasing amount of zinc(II) added the intensity of the ligand band at 435 nm diminishes, while a new band at 375 nm grows progressively, and all the absorption curves pass through the isosbestic points at 395 and 345 nm. The spectrum obtained after addition of 2 equiv of $Zn(OAc)_2 \cdot 2H_2O$ is identical to that of **12**. The smooth changeover of the ligand spectrum to that of **12** on addition of zinc(II) indicates simultaneous occupation of the two cavity sites of the macrocycle by the metal ions according to eq 5.

$$[H_4L^3]^{2+} + 2Zn(OAc)_2 \rightleftharpoons [Zn_2L^3(\mu\text{-}OAc)]^{+} + H^{+} + 3HOAc \quad (5)$$

Spectrofluorimetric Titrations of $[H_4L^{1-3}](ClO_4)_2$ with $Zn(OAc)_2 \cdot 2H_2O$. We have recently reported[17] that the macrocyclic ligands $[H_4L](ClO_4)_2$ with the lateral side chains varying from $-(CH_2)_2-$ to $-(CH_2)_{12}-$ all exhibit photoluminescence in solution at room temperature. However, there are considerable differences in the fluorescence intensities of these compounds across the series. For example, the acetonitrile solutions (1×10^{-5} M) of $[H_4L^{1-3}](ClO_4)_2$ on excitation at 440−450 nm fluoresce at 500−510 nm, and their normalized intensities (in arbitrary units) decrease in the order L^3 (960) > L^1 (145) > L^2 (3).

Spectrofluorimetric titrations were carried out by adding an incremental amount (0.2 equiv) of an acetonitrile solution of $Zn(OAc)_2 \cdot 2H_2O$ (1×10^{-3} M) to a solution of the ligand (1×10^{-5} M) in the same solvent and monitoring either the growth of the luminescent band due to complex formation/or the depletion of the ligand emission band due to its consumption.

The growth of the emission band at 435 nm with the addition of zinc(II) to $[H_4L^2]^{2+}$ using 370 nm (λ_{max} for the dizinc(II) complex) as the excitation wavelength is shown in Figure 6. The shape of the curve indicates that, while complex formation takes place in a stepwise manner, considerable overlapping occurs between the two steps. The observation made during spectrophotometric titration is consistent with this conclusion.

Figure 7 shows that the luminescence band of $[H_4L^3]^{2+}$ observed at 500 nm (with λ_{ex} = 440 nm) progressively

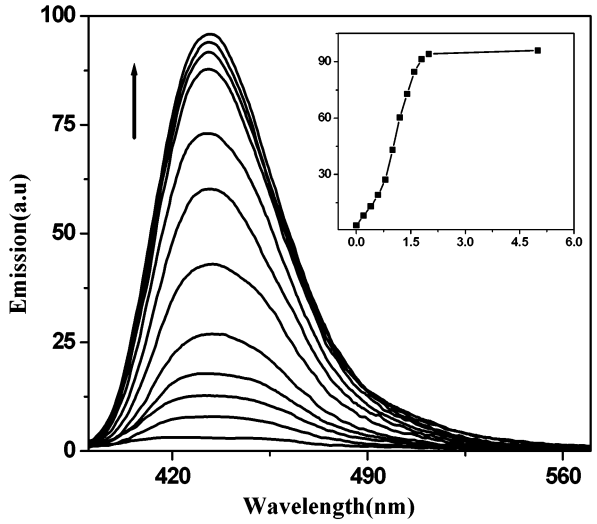

Figure 6. Spectrofluorimetric titration of the macrocycle $[H_4L^2](ClO_4)_2$ (1×10^{-5} M) with various numbers of equivalents of $Zn(OAc)_2 \cdot 2H_2O$ in acetonitrile. The arrow ↑ indicates the increasing concentration of $Zn(OAc)_2 \cdot 2H_2O$ added. $\lambda_{ex} = 370$ nm. The inset shows the variation of luminescence intensity with the number of equivalents of $Zn(OAc)_2 \cdot 2H_2O$ added.

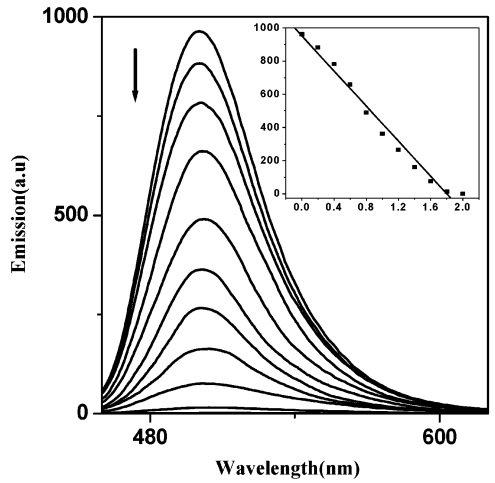

Figure 7. Spectrofluorimetric titration of the macrocycle $[H_4L^3](ClO_4)_2$ (1×10^{-5} M) with various equivalents of $Zn(OAc)_2 \cdot 2H_2O$ in acetonitrile. The arrow ↓ indicates the increasing concentration of $Zn(OAc)_2 \cdot 2H_2O$ added. $\lambda_{ex} = 440$ nm. The inset shows the variation of luminescence intensity with the number of equivalents of $Zn(OAc)_2 \cdot 2H_2O$ added.

becomes quenched on incremental addition of zinc(II) and finally vanishes when the ligand-to-metal ratio (L:M) becomes 1:2. The diminution of the luminescence intensity plotted against the number of equivalents of zinc(II) added provides a straight line (shown in the inset of Figure 7) to indicate that in this case the formation of the dizinc(II) complex occurs in a single step. Conversely, if the growth of the luminescence band of the complex observed at 438 nm (with $\lambda_{ex} = 370$ nm) is monitored as a function of the amount of zinc(II) again a linear relationship is obtained.

In the case of titration of $[H_4L^1]^{2+}$ with zinc acetate, the decrease in intensity of the emission band of the ligand at 510 nm (with $\lambda_{ex} = 440$ nm) and the increase in intensity of the emission band due to complex formation at 450 nm (with $\lambda_{ex} = 370$ nm) were monitored. The variation of emission intensities at 510 and 450 nm with the number of equivalents of zinc acetate added is shown in Figure 8. In both the cases,

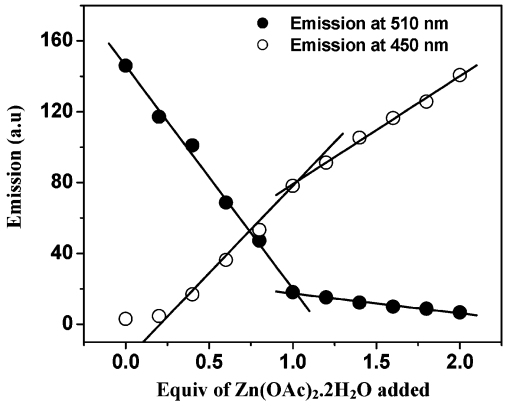

Figure 8. Variation of emission intensity during titration of the macrocycle $[H_4L^1](ClO_4)_2$ (1×10^{-5} M) with various numbers of equivalents of $Zn(OAc)_2 \cdot 2H_2O$ in acetonitrile. Solid circles represent emission at 510 nm with $\lambda_{ex} = 440$ nm; open circles represent emission at 450 nm with $\lambda_{ex} = 370$ nm.

Table 5. Absorption and Emission Spectral Data for Complexes **1**−**12**

		absorption	emission[a]	
compd	solvent	λ_{max}, nm (ϵ, $M^{-1}\,cm^{-1}$)	λ_{em}, nm	φ
1	acetonitrile	402 (15600), 247 (72600)		
2	acetonitrile	370 (13900), 251 (76800)	450	
3	methanol	370 (16900), 251 (78200)	427	0.031
	acetonitrile	370 (16600), 250 (77300)	431	0.027
4	methanol	370 (15700), 250 (70900)	429	0.039
	acetonitrile	370 (15900), 251 (75300)	433	0.035
5	methanol	370 (17900), 250 (85300)	428	0.046
	acetonitrile	370 (17000), 252 (84000)	432	0.043
6	methanol	370 (18400), 251 (85800)	428	0.047
	acetonitrile	370 (18400), 250 (84900)	433	0.048
7	methanol	370 (18800), 250 (88600)	429	0.047
	acetonitrile	369 (18300), 254 (88200)	433	0.046
8	methanol	370 (19000), 251 (89000)	428	0.044
	acetonitrile	371 (18900), 250 (86000)	432	0.042
9	methanol	370 (15400), 252 (73000)	427	0.021
	acetonitrile	370 (15900), 252 (75100)	433	0.018
10	acetonitrile	369 (18000), 254 (91800)	433	
12	acetonitrile	377 (10400), 254 (402000)	438	

[a] Excitation wavelength 370 nm.

the observed data can be best represented by two sets of straight lines differing in slope which intersect at the point when L:M is 1. This observation substantiates why, unlike L^2 and L^3, it has been possible to isolate both the mononuclear (**1**) and dinuclear (**2**) complexes of L^1.

Emission Spectra of 4−9. The luminescence spectra of the carboxylate-bridged complexes **4**−**9** were measured in methanol and acetonitrile solutions (1×10^{-5} M) at room temperature. Table 5 summarizes the absorption and emission spectral characteristics of the complexes, including their quantum yields. Similar to the precursor complex $[Zn_2L^2(H_2O)_2]^{2+}$, complexes **4**−**9** all exhibit an absorption band at 370 nm, the position of which remains the same in methanol and acetonitrile. Accordingly, with 370 nm as the excitation wavelength, the emission peak is observed at about 430 nm for all the complexes. For the sake of comparison, the emission spectra recorded for **3**−**9** in acetonitrile are shown in Figure 9. It may be noted that, relative to that of **3**, the fluorescence intensity of the acetate complex **4** is stronger (by a factor of 1.2). In the case of the benzoate complex **5**, further intensification of the emission band occurs (1.4 times stronger relative to that of **3**). Subtle electronic

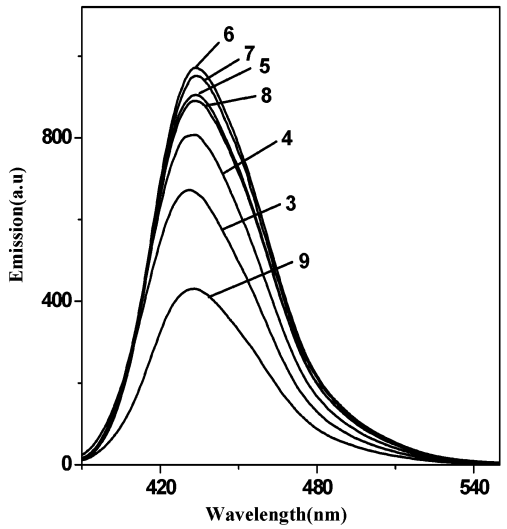

Figure 9. Relative luminescence intensities observed for the carboxylate-bridged complexes **4**−**9** with respect to **3** in acetonitrile (concentration 1 × 10^{-5} M).

influence of the *para*-substituents is observed for **6** (Me) > **7** (OMe) > **8** (Cl). Significantly, with the strongly electron-withdrawing *p*-nitro group in **9**, substantial reduction of fluorescence intensity occurs (1.5 times less relative to that of **3**).

Equilibrium Constants. The equilibrium constants for the reaction

$$[Zn_2L^2(H_2O)_2]^{2+} + A^- \overset{K}{\rightleftharpoons} [Zn_2L^2A]^+ + 2H_2O \qquad (6)$$

involving the dinuclear zinc(II) complex **3** and the carboxylate anions (A^-) derived from sodium acetate and benzoate and a number of amino acids (such as glycine, L-alanine, L-histidine, L-valine, and L-proline) which exist in the zwitterionic form $RN^+H_2 \sim\!\sim CO_2^-$ were determined by spectrofluorimetric titrations in aqueous solution. No buffer was used in these measurements to avoid any possible interference by its constituents (for example, carboxylate or phosphate). Nevertheless, at the level of concentration of the solutions ($\sim 10^{-5}$ M) used, the pH of the solutions remained between 6.4 and 6.8. Typical changes in the luminescence spectrum of an aqueous solution (1 × 10^{-5} M) of $[Zn_2L^2(H_2O)_2]^{2+}$ with varying amounts of L-alanine (1 × 10^{-6} to 3 × 10^{-5} M) are shown in Figure 10. The emission peak of **3** at 425 nm (λ_{ex} = 370 nm) grows in intensity with increasing amount of alanine and reaches the maximum when its concentration is 2 × 10^{-5} M. When **3** is titrated with sodium benzoate solution, a similar observation (shown in Figure S6 in the Supporting Information) is made. Since in this case (also for acetate) 1:1 complex formation occurs, it is reasonable to expect a similar type of interaction with the amino acids. Indeed, it has been structurally established that the dinickel(II) macrocyclic analogue forms μ-carboxylato complex species with glycine etc. in the zwitterionic form.[26,27]

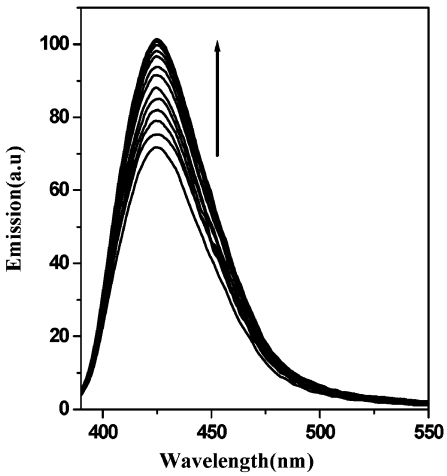

Figure 10. Spectrofluorimetric titration of $[Zn_2L^2(H_2O)_2](ClO_4)_2$ (1 × 10^{-5} M) with increasing concentration (↑) of L-alanine (1 × 10^{-6} to 3 × 10^{-5} M) in water. λ_{ex} = 370 nm.

The equilibrium constants (*K*) were evaluated by linear regression analysis, and the values thus obtained are 2.8(2) × 10^5 for acetate, 1.2(2) × 10^5 for benzoate, 2.5(3) × 10^5 for alanine, 3.1(2) × 10^5 for histidine, 4.4(4) × 10^5 for valine, and 8.0(5) × 10^5 for proline. It is interesting to note that the binding constants obtained for the amino acids do not differ much among themselves and also are of the same orders of magnitudes as those of acetate and benzoate. Clearly, in all the cases a similar mode of substrate binding is involved.

Conclusion. The binding of zinc(II) with the macrocyclic ligands $[H_4L^{1-3}]^{2+}$, whose cavity sizes increase progressively, have been studied by spectrophotometric and spectrofluorimetric titrations. Stepwise complexation occurs in the case of L^1, making it possible to isolate both the mononuclear (**1**) and dinuclear (**2**) complexes. In the case of L^2, the two successive equilibria overlap considerably, and therefore, only the dinuclear complex **3** could be isolated. As such, L^3 fails to complex with zinc(II); however, in the presence of acetate the formation of $[Zn_2L^3(\mu\text{-OAc})]^+$ takes place in a single step. Complexes **3** and **12** have been structurally characterized. The reaction between **3** and an excess of acetate/benzoate produces complexes **4**−**9**. Significantly, the benzoate complex **5** on reaction with benzoic acid produces a compound of unusual composition, **10**. The crystal structure determination of **10** indicates that protonation occurred to the coordinated water molecule. The structural consequence of this unusual binding is the drainage of electron density from the Zn(1) coordination sites to the Zn(2) sites, and as a result Zn(1)−O bond distances are shorter relative to Zn(2)−O distances. Importantly, complex **10** on treatment with 1 equiv of sodium hydroxide produces the neutral dibenzoate complex **11**, whose formation provides support to the presence of H_3O^+ ion in **10**. The photoluminescence behavior studied for complexes **4**−**9** indicates that the intensities of the luminescence spectra vary with the donor ability of the carboxylate; it is maximum for the *p*-methyl derivative (**6**) and minimum for the *p*-nitro derivative (**9**). The equilibrium constants (*K*) involving the binding of acetate/benzoate and the carboxylate moiety of five amino acids with $[Zn_2L^2(H_2O)_2]^{2+}$ have been determined in aqueous

(26) Das, R.; Nanda, K. K.; Venkatsubramanian, K.; Paul, P.; Nag, K. *J. Chem. Soc., Dalton. Trans.* **1992**, 1253.
(27) Nanda, K. K.; Das, R.; Thompson, L. K.; Venkatsubramanian, K.; Nag, K. *Inorg. Chem.* **1994**, *33*, 5934.

solution by spectrofluorimetric titrations. The values of K lying in the range $(1-8) \times 10^5$ indicate that the amino acids are quite effective in binding with the zinc fluorophore through their carboxylate unit.

The significant aspect of this study is the observation of zinc-induced fluorescence enhancement of the macrocyclic ligand $[H_4L^2](ClO_4)_2$, which can be considered as a photoinduced charge-transfer fluorophore. The internal charge transfer (ICT) that occurs from the phenolate donor site to the protonated imino acceptor site of the ligand at 440 nm undergoes a blue shift to 370 nm on formation of the dizinc(II) complex $[Zn_2L^2(H_2O)_2]^{2+}$. Consequently, the luminescence band of the ligand at 510 nm is also markedly blue-shifted to 435 nm with considerable enhancement of intensity. The 70-fold increase in luminescence intensity of $[Zn_2L^2(H_2O)_2]^{2+}$ relative to $[H_4L^2](ClO_4)_2$ is further augmented with the formation of the carboxylate-bridged complexes $[Zn_2L^2(\mu\text{-}O_2CR)]^+$.

Acknowledgment. We are thankful to the Department of Science and Technology, Government of India, for providing funds to purchase the spectrofluorimeter of the Department of Inorganic Chemistry of the Indian Association for the Cultivation of Science.

Supporting Information Available: X-ray crystallographic files in CIF format for compounds **3**, **10**, and **12** and Figures S1−S6 (PDF). This material is available free of charge via the Internet at http://pubs.acs.org.

IC049056A